Influence of Suction and Porous Medium on MHD Thermal Transport of a Non-Newtonian Ternary Hybrid Nanofluid over a Nonlinearly Stretching Surface

Muhammad Ramzan[1], Aamir Shahzad[2]*, Sidra Ashraf[3]
[1]Faculty of Sciences, Superior University Lahore, Lahore, Pakistan
[2]Department of Mathematics, Faculty of Natural Sciences and Technology, Baba Guru Nanak University, Nankana Sahib, Pakistan
[3]Department of Mathematics, Faculty of Sciences, University of Sargodha, Sargodha, Pakistan
***Correspondence:** aamir.shahzad@bgnu.edu.pk,

Citation | Ramzan. M, Shahzad. A, Ashraf. S, "Influence of Suction and Porous Medium on MHD Thermal Transport of a Non-Newtonian Ternary Hybrid Nanofluid over a Nonlinearly Stretching Surface", IJIST, Vol. 8 Issue. 6 pp 2517-2530, September 2026
DOI: https://doi.org/10.33411/IJIST/2006
Received | Aug 10, 2026 Revised | Sep 02, 2026 Accepted | Sep 05, 2026 Published | Sep 08, 2026.

This study investigates the momentum and thermal transport characteristics of a ternary hybrid non-Newtonian Maxwell fluid containing spherical Ag–Cu–TiO_2 nanoparticles dispersed in kerosene oil. The flow is considered over a nonlinearly stretching flexible sheet embedded in a porous medium under the combined effects of wall suction, an externally applied magnetic field, and buoyancy. Appropriate similarity transformations are employed to reduce the governing nonlinear partial differential equations for momentum and energy into a coupled system of ordinary differential equations, which is subsequently solved numerically using the MATLAB bvp4c solver. The effects of the Maxwell relaxation parameter, magnetic parameter M, buoyancy parameter λ, Prandtl number Pr, porous-medium parameter K, suction parameter S, and inclination angle ξ are systematically examined. The numerical results demonstrate that increasing M suppresses the velocity field while enhancing the temperature distribution because of the increased Lorentz-force resistance. Over the investigated magnetic-parameter range, the velocity decreases, whereas the temperature increases. Increasing the porous-medium parameter K similarly reduces the velocity and enhances the temperature distribution; quantitatively, the corresponding changes, respectively. In contrast, increasing the Maxwell relaxation-time parameter enhances the velocity throughout the boundary layer, while increasing the inclination angle from ξ=0 to $\pi/2$ produces a continuous acceleration of the flow. The Ag/kerosene-oil nanofluid exhibits a consistently higher velocity than the Ag–Cu/kerosene-oil hybrid nanofluid, whereas the latter produces a higher temperature distribution. The surface-transport characteristics further reveal that increasing K raises the wall shear-stress coefficient and reduces the Nusselt number. Likewise, increasing Pr enhances the wall shear coefficient, while the reduced Nusselt number decreases accordingly. Stronger wall suction further restricts the thermal boundary-layer thickness. These findings demonstrate that magnetic forcing, porous-medium resistance, viscoelastic relaxation, inclination, suction, and thermal diffusivity provide effective mechanisms for controlling momentum and heat transfer in nanoparticle-enhanced Maxwell fluids, highlighting their potential for advanced thermal-management and energy-conversion applications.

Keywords: Tri-hybrid particles, Kerosene oil, Non-linear, Permeable medium.

Introduction:

Ternary hybrid nanofluids represent an advanced class of heat-transfer fluids formed by dispersing three distinct types of nanoparticles within an appropriate base fluid, such as water and biological fluids including blood etc. These improvements are primarily attributed to the combined and synergistic effects of the three different nanoparticle components uniformly dispersed throughout the base fluid. Owing to these advantages, they have attracted increasing attention for applications in advanced cooling technologies, thermal-management systems, renewable energy devices, heat exchangers, and various industrial heat-transfer processes.

In recent years many researchers have been working on tri-hybrid nanofluidswith different properties like for unsteady water-based ternary hybrid nanofluid transport over wedge-type geometries with bioconvection and wall stretching was studied by [1]. Their formulation extended THNF modeling to geothermal and bio-convective thermal systems by highlighting the significance of nanoparticle thermal conductivity, unsteadiness, and the motion of gyrotactic microorganisms in regulating momentum, heat, and mass transmission. Within a similar magnetohydrodynamic paradigm SiO_2–TiO_2–AlO_3/water ternary hybrid nanofluid flow across a stretching sheet in the presence of a magnetic dipole and nonlinear thermal radiation was studied by [2]. The work confirmed the value of multicomponent nanoparticle suspensions for regulated energy-transfer processes and showed the great sensitivity of thermal transport to magnetic and radiative mechanisms by contrasting nano-, hybrid-, and ternary-hybrid configurations. [3] highlighted the significant role of nanopartices in governing the heat-transfer characteristics of nanofluids. For radiator cooling, [4] examined a water-based ternary system with carbon nanotubes, graphene nanoparticles, and variously shaped Al2O3. The potential of THNFs in cutting-edge automotive and industrial cooling systems is supported by their fractional-model analysis, which revealed that the ternary hybrid formulation performed better in heat transfer than equivalent hybrid and unitary nanofluids. By investigating ternary-hybrid nanofluids through a convergent-divergent nozzle using distilled water–ethylene glycol base-fluid mixes, [5] expanded this idea to internal-flow applications. Their theoretical studies further demonstrated the adaptability of ternary systems to various heat-transfer configurations by proving that base-fluid composition and nanoparticle loading can significantly affect the thermo-fluid characteristics of nozzle flow. By adding optimization, permeable geometries, non-Newtonian effects, fractional calculus, and entropy analysis, more recent studies have expanded the scope of THNF study. Cu–TiO_2–SiO_2/water ternary hybrid nanofluid flow across a symmetrically extending sheet was investigated by [6], who combined the mathematical solution with a support-vector-machine prediction scheme. The work demonstrates a significant shift in the area from strictly numerical simulation to data-driven prediction, where complicated THNF systems' response may be effectively estimated by machine-learning algorithms across a broad range of operating parameters. The thermal behavior of tri-hybrid nanoliquid flow past a permeable inclined cylinder/plate was studied by [7]. [8] further extended the application of ternary hybrid nanofluids to biomedical heat-transfer systems by examining the unsteady flow of a couple-stress Casson tri-hybrid nanofluid containing differently shaped Fe_3O_4, Zn, and Au nanoparticles dispersed in blood using the Atangana–Baleanu fractional operator. [9] investigated Marangoni-driven flow of a tri-hybrid nanofluid with particular emphasis on entropy generation and irreversibility. Similarly in a related investigation, [10] examined the natural-convection characteristics of an Al_2O_3–Ag–CuO/water ternary hybrid nanofluid within a differentially heated enclosure subjected to non-uniform wall heating. [11] examined entropy generation and hydrothermal optimization of a polymer-based tri-hybrid nano-liquids over a curved sheet. By simultaneously considering heat-transfer performance and

irreversibility, their study highlighted the importance of balancing thermal enhancement against entropy production when selecting operating conditions for advanced thermal devices. [12] examined chemically reactive MHD convective flow of a Cu–TiO_2–Al_2O_3/water tri-component nano liquids over a curved stretching sheet. The work confirmed that strong connections between momentum, energy, and species-transport mechanisms drive THNF behavior by showing how the coupled thermal, magnetic, and chemical characteristics significantly affect velocity, temperature, and concentration distributions. In order to demonstrate how wall mass transfer, slip conditions, magnetic effects, and stretching or shrinking kinematics may be controlled to control boundary-layer behavior and heat transport, [13] concentrated on slip flow of a ternary hybrid nanofluid with suction over a stretching/shrinking sheet. Because suction offers a direct method of regulating boundary-layer thickness and maintaining heat-transfer properties in surface-driven flows, its inclusion is especially pertinent. For MHD Carreau ternary hybrid nanofluid flow across a vertical cylinder, [14] integrated artificial neural-network analysis with numerical calculation. Their findings showed that the introduction of ternary nanoparticles increases the heat-transfer rate, while the neural-network component demonstrates the growing value of intelligent surrogate models for predicting highly nonlinear heat- and mass-transfer responses. Most recently, [15] used thermophoretic particle deposition, thermal radiation, activation energy, and chemical reaction to study MHD heat and mass transfer of a Cu–Fe_3O_4–ZrO_2/propylene-glycol ternary hybrid nanofluid over a spinning sphere. According to their findings, the ternary system outperforms the corresponding hybrid formulation thermally; increasing the volume fraction of nanoparticles improves heat transfer but also increases viscous resistance; and stronger magnetic interaction suppresses velocity thru the Lorentz force while increasing the thermal field.

In 2022 [16] studied an electrically conducting ternary hybrid nanofluid containing TiO_2, cobalt ferrite and MgO nanoparticles dispersed in water over an extending cylindrical surface. The formulation incorporated magnetic-induction effects and Darcy-type resistance, allowing the authors to examine how electromagnetic and porous-medium mechanisms alter momentum and thermal transport. The work is important because it moved ternary hybrid nanofluid modeling beyond flat stretching sheets and into cylindrical boundary-layer configurations, which are relevant to wire coating, fiber processing and tubular thermal systems. Its overall contribution is the demonstration that combining three nanoparticles with magnetic control provides an additional degree of freedom for tailoring velocity and heat-transfer behavior, while also increasing the complexity of the effective thermophysical-property model. In the same year [17] analyzed unsteady electro-viscous ternary hybrid nanofluid flow between parallel plates while simultaneously accounting for chemical reaction and Arrhenius activation energy. In 2023 [18] and [19] investigated a Jeffrey ternary hybrid nanoliquid over a convectively heated porous curved surface and examined tri-hybrid nanofluid flow over a stretching surface with a heat source and thermal-slip effects respectively. [20] developed a fractal-fractional model for natural-convection heat transfer of a ZnO–Al_2O_3–TiO_2/distilled-water ternary hybrid nanofluid in a vertical channel.

In 2024, many authors including Shah et al., Mahboobtosi et al. and Wahid et al. worked on tri-hybrid nanofluids with chemical mixing. These studies are important regarding tri-hybrid type fluids. For example, [21] analyzed Maxwell-fluid flow containing ternary hybrid nanoparticles over a Riga plate under convective boundary conditions. [22] compared ternary hybrid nanofluids with conventional single nanofluids around a stretched cylinder under porous-medium, magnetic-field, thermal-radiation, viscous-dissipation and Darcy–Forchheimer effects and [23] investigated unsteady water-based Al_2O_3–Cu–TiO_2 ternary hybrid nanofluid flow over a permeable biaxial shrinking sheet with thermal radiation.

Recently, [24] modeled TiO_2–Al_2O_3–SiO_2 ternary hybrid nanofluid flow over a stretching/shrinking wedge using a modified Buongiorno formulation, activation energy and endothermic/exothermic chemical-reaction effects. [25] examined entropy generation in magnetized tri-hybrid nanofluid flow over a curved stretching surface in a variable Darcy–Forchheimer medium. Similarly, [26] investigated convective heat transfer of a tri-hybrid nanofluid over a curved expanding surface with velocity slip, magnetic effects and an exponential heat source. also [27] studied two-dimensional Darcy–Forchheimer ternary hybrid nanofluid flow over a curved (bended) surface using active and passive nanoparticle-control conditions. [28] explored a non-Newtonian ternary hybrid nanofluid model with homogeneous–heterogeneous chemical reactions associated with flow induced by a vertical cylinder. A combined mathematical modeling with fuzzy particle swarm optimization and artificial neural networks to predict heat-transfer behavior in a ternary hybrid nanofluid was also studied by [29]. The work considered a non-Newtonian flow involving Al_2O_3, graphene and CNT nanoparticles and used the soft-computing models to estimate the Nusselt number over a range of governing parameters. The reported very small prediction errors and high correlation values demonstrated that AI-based surrogates can reproduce the numerical solution with high accuracy within the training domain. This study is significant because it shifts the emphasis from merely solving a ternary nanofluid model to building predictive tools that can support parameter optimization and rapid design-space exploration.

In 2025, [30] analyzed MHD ternary hybrid nanofluid flow through a porous medium over a rotating stretching sheet with thermochemical reactions and activation energy and [31] examined transient Carreau ternary hybrid nanofluid flow over a stretching sheet under electromagnetic and thermal effects, with emphasis on entropy generation and regression analysis.

Collectively, studies[1] [2] [3] [4] [5] [6] [7] [8] [9] [10] [11] [12] [13] [14] [15] [16] [17] [18] [19] [20] [21] [22] [23] [24] [25] [26] [27][28] [29] [30] [31] demonstrate that ternary and tri-hybrid nanofluids offer considerable potential for enhancing thermal transport across stretching surfaces, wedges, nozzles, cylinders, curved sheets, enclosures, channels, and rotating geometries. The literature also shows a clear evolution from basic heat-transfer enhancement toward multi-physics models involving MHD effects, porous media, nonlinear radiation, chemical reaction, suction, slip, non-Newtonian rheology, entropy generation, fractional operators, and machine-learning prediction. However, the simultaneous interaction of complicated stretching kinematics, suction, magnetic forces, non-Newtonian properties, and porous-medium resistance is still very poorly integrated into a single modeling framework. This offers a solid foundation for future research on MHD non-Newtonian ternary hybrid nanofluid transport under combined suction and porous-medium effects, especially in situations where high-performance cooling, energy conversion, and industrial thermal-management applications demand precise control of momentum and thermal boundary layers.

Objective of the Study:

The main objective of the present study is to investigate the hydrothermal characteristics of an Ag–Cu–TiO_2/kerosene-oil ternary hybrid nanofluid within the framework of a Maxwell non-Newtonian fluid model, with particular emphasis on the combined effects of magnetic forcing, wall suction, porous-medium resistance, and fluid relaxation. The study is designed to clarify how the interaction of these mechanisms modifies the momentum and thermal boundary layers and, consequently, the overall heat-transfer performance of the ternary hybrid nanofluid system. More specifically, the objectives of the present investigation are:

To formulate and analyze the flow and heat-transfer characteristics of Ag–Cu–TiO_2 nanoparticles dispersed in kerosene oil using the Maxwell-fluid constitutive model.

To determine the influence of the magnetic-field parameter on the fluid velocity and temperature distributions and to quantify the associated changes in momentum and heat transport caused by the Lorentz force.

To investigate the effect of the suction parameter on boundary-layer thickness, velocity distribution, temperature field, and surface heat-transfer characteristics, with particular attention to its capability to regulate momentum and thermal transport near the surface.

To evaluate the effects of the other governing thermophysical and dimensionless parameters incorporated in the mathematical formulation on the velocity and temperature profiles and on the relevant engineering quantities, including the skin-friction coefficient and Nusselt number.

Through these objectives, the present study aims to provide a systematic understanding of the individual and combined roles of magnetic, porous, suction, non-Newtonian, and nanoparticle-related effects in controlling the flow and thermal performance of the proposed ternary hybrid nanofluid.

Research Novelty:

The novelty of the present investigation lies in the development and analysis of an Ag–Cu–TiO_2/kerosene-oil ternary hybrid nanofluid model incorporating Maxwell-fluid rheology together with magnetic-field effects, wall suction, and porous-medium resistance. Although considerable attention has been given to conventional nanofluids, binary hybrid nanofluids, and more recently ternary hybrid nanofluids, comparatively limited attention has been directed toward the combined influence of non-Newtonian relaxation behavior, magnetohydrodynamic forcing, suction, and porous-medium resistance in an Ag–Cu–TiO_2 ternary nanoparticle suspension using kerosene oil as the base fluid. Previous ternary hybrid nanofluid studies have largely concentrated on water- or water/ethylene-glycol-based suspensions, Newtonian flow models, or different combinations of nanoparticles and surface configurations. In contrast, the present formulation considers the simultaneous incorporation of three thermally conductive nanoparticles—silver (Ag), copper (Cu), and titanium dioxide (TiO_2)—into kerosene oil, while retaining the relaxation characteristics of a Maxwell fluid. This combination enables the interaction between nanoparticle-induced thermal enhancement and the elastic nature of the carrier fluid to be investigated under magnetic and porous-medium effects.

The unresolved research gap addressed in this work is consequently the lack of a unified analysis of Ag–Cu–TiO_2/kerosene ternary hybrid nanofluid transport under the simultaneous influences of Maxwell-fluid relaxation, an externally imposed magnetic field, surface suction, and porous-medium resistance. By examining the effects of the magnetic parameter, suction parameter, porous-medium parameter, Maxwell parameter, nanoparticle loading, and the remaining governing transport parameters within a single mathematical framework, the study provides a more comprehensive description of the coupled hydrodynamic and thermal behavior of the system. The findings are expected to contribute to the design and optimization of advanced thermal-management processes in which enhanced heat transfer must be balanced against increased momentum resistance.

The initial phenomenon of the proposed formulations:

The present study aims to investigate the thermal performance of Ag–Cu–TiO_2 nanoparticles dispersed in kerosene oil under magnetohydrodynamic (MHD) Maxwell fluid flow. A tri-component based non-Newtonian Maxwell flow model is employed to evaluate the influence of spherical nanoparticles on the heat-transfer characteristics of the base fluid over a nonlinearly stretching sheet subjected to porous suction. Particular emphasis is placed on the effects of key governing parameters, including mass flux and porous-medium characteristics. Figure 1 illustrates the complete flow structure using a flow diagram. The flow

equations by following;

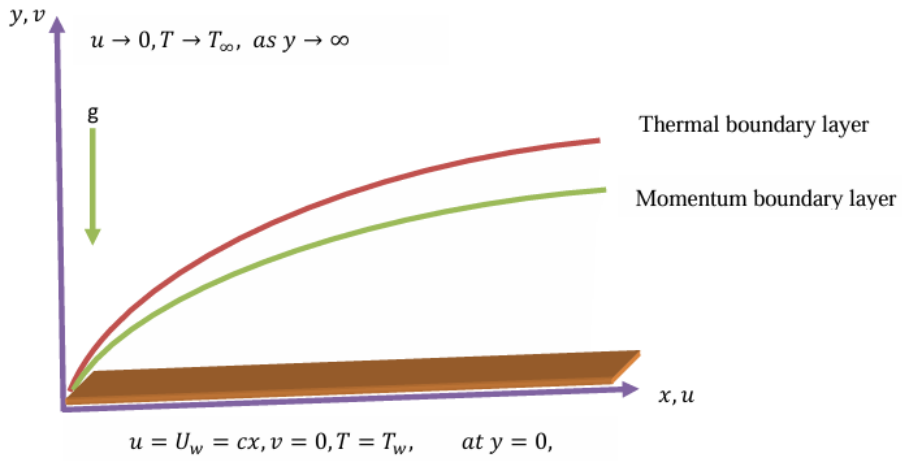

Figure. 1 Flow Structure

Underlying Mathematical Theory:

A steady, 2D laminar type flow of a tri-hybrid nano-liquids over a flexible surface is investigated in the presence of a uniform transverse magnetic field, suction, and a porous medium. The equations describing the momentum and thermal transport features of the proposed flow system are observed as follows:

$$\frac{\partial u_1}{\partial x} + \frac{\partial u_2}{\partial y} = 0, \tag{1}$$

$$\left(u_1 \frac{\partial u_1}{\partial x} + u_2 \frac{\partial u_1}{\partial y}\right) = \frac{\mu_{thnf}}{\rho t_{hnf}} \frac{\partial^2 u_1}{\partial y^2} - \frac{\beta}{\rho_{thnf}} \left(u_1{}^2 \frac{\partial^2 u_1}{\partial x^2} + u_2{}^2 \frac{\partial^2 u_1}{\partial y^2} + 2u_1 u_2 \frac{\partial^2 u_1}{\partial x \partial y}\right) - \frac{g(\rho\beta_T)_{thnf}}{\rho t_{hnf}} (T - T_\infty) + \frac{\sigma_{thnf}}{\rho_{thnf}} B_o^2 u_1 - \frac{\nu_{thnf}}{K_o} u_1 , \tag{2}$$

$$\left(\rho C_p\right)_{thnf} \left(u_1 \frac{\partial T}{\partial x} + u_2 \frac{\partial T}{\partial y}\right) = k_{thnf} \frac{\partial^2 T}{\partial y^2}. \tag{3}$$

Now (1-3) are composed with boundary conditions as

$$u_1\,(x, 0) = \mathrm{U_w}(x) = \mathrm{U_0} e^{\frac{x}{L}}\ , u_2 = -(u_2)_o\ , T(x, 0) = T_w\ , C(x, 0) = C_w \quad at\ \ y = 0$$
$$u_1 \to 0, T \to T_\infty, C \to C_\infty. \tag{4}$$

The velocity components in these formulations are shown by cartesian coordinates x and y. The magnitudes T, Tw, and T∞ denote the fluid temperature, wall temperature, and ambient fluid temperature, respectively. Similarly, C, C_w, and C_∞ correspond to the solute concentration within the fluid, at the wall surface, and in the ambient fluid, respectively.

Numerical Solution Technique:

This section presents the solution methodology employed to solve the governing equations (1–3) subject to the boundary conditions given in expression (4). Initially, appropriate similarity transformations are introduced to transform the governing PDEs into a corresponding system of ODEs. Subsequently, the numerical technique adopted to solve the resulting nonlinear ODE system is described, together with the transformed boundary conditions.

Coordinate Transformation Method:

In this section, the similarity transformations defined in equation (5) are employed to convert the coupled nonlinear PDEs (1–3), together with the associated fluid constraints given in (4), into an ODE system. The similarity variables are defined as follows:

$$u_1 = U_0 e^{x/L}\,\psi'(\eta), u_2 = -\sqrt{\frac{vU_0}{2L}}\,e^{x/2L}[\,\psi(\eta) + \eta\psi'(\eta)]$$
$$\varphi = \sqrt{2vLU_0}\,e^{x/2L}\psi(\eta), \qquad \chi(\eta) = \frac{T - T_\infty}{T_o - T_\infty}, \eta = \sqrt{\frac{U_0}{2vL}}\,ye^{x/2L} \Bigg\} \tag{5}$$

Upon introducing the similarity transformations given in (5) into (1–4), then (1) is identically satisfied, and the resulting residual expressions can be expressed as follows:

$$\frac{\frac{\mu_{thnf}}{\mu_f}}{\frac{\rho_{thnf}}{\rho_f}}\psi''' - 2\psi'^2 - \psi\psi'' - \frac{\lambda_1}{\frac{\rho_{thnf}}{\rho_f}}\left(\psi^2\psi''' - 2\psi\psi'\psi''\right) - \frac{\frac{(\rho\beta_T)_{thnf}}{(\rho\beta_T)_f}}{\frac{\rho_{thnf}}{\rho_f}}\lambda\chi - \frac{\frac{\sigma_{thnf}}{\sigma_f}}{\frac{\rho_{thnf}}{\rho_f}}M\psi' -$$
$$\frac{\mu_{thnf}}{\mu_f}K\psi' = 0, \tag{6}$$

$$\frac{\frac{k_{thnf}}{k_f}}{\frac{(\rho C_P)_{thnf}}{(\rho C_P)_f}}\frac{1}{Pr}\theta'' + (\psi\chi' - \psi'\chi) = 0 \tag{7}$$

Considered boundary constraints

$$\left.\begin{array}{l}\psi = S,\ \psi' = 1,\ \theta = 1,\ \text{at}\,\eta = 0\\ \psi' \to 0,\ \chi \to 0,\ \text{as}\,\eta \to \infty\end{array}\right\}, \tag{8}$$

Where, $\lambda_1 = \frac{\beta U_0}{\rho_f L}$ is viscoelastic relaxation parameter, with β as relaxation parameter of time, $\lambda = \frac{g(\beta_T)_f \Delta T}{C^2 x}$ is thermal buoyancy coefficient with $\Delta T = (T_w - T_\infty)$, $M = \frac{\sigma_f B_{0L}^2}{U_0 \rho_f}$ is Lorentz number, $K = \frac{\nu_f L}{K_o U_0}$ is dimensionless porosity parameter, $Pr = \frac{\nu_f}{\alpha_f}$ is thermal boundary layer number with $\alpha = \frac{k_f}{(\rho C_P)_f}$ as heat penetration rate, $S = \frac{v_o}{\sqrt{U_0 \nu_{f/2L}}}$ is negative flux parameter $(v_o > 0)$. Here, η be known as variable of similarity.

Principal engineering parameters:

The key parameters of primary interest are the skin-friction coefficient and the Nusselt number, which are expressed as

$$C_f = \frac{\mu_{thnf}}{\rho_{thnf}}\sqrt{1/2vLU_0 e^{x/L}}\,\psi''(0), \mathrm{Nu}_x = x\sqrt{\frac{U_0}{2vL}}\,ye^{x/2L}\,(-\chi'(0)) \tag{9}$$

Incorporating Equation (5) into Equation (9), followed by appropriate algebraic manipulation, yields

$$Re_x^{1/2} C_f = \sqrt{\frac{\mu_{thnf}}{2\rho_{thnf}\nu_{thnf}}} \qquad \psi'', (0), Re_x^{-1/2}\mathrm{Nu}_x = -\frac{x}{2L}\chi'(0) \tag{10}$$

Where, $Re_x = \mathrm{U_w}L$ is the spatial dimensionless flow parameter. In the following Table 1, heat–f' vf transport and physical properties of the primary fluid kerosene oil, Ag–Cu and $TiO2$ are given.

Table 1. Thermal-physical attributes [32]

Properties	$\rho(Kg/m)$	C_p ($JKg^{-1}K^{-1}$	k ($Wm^{-1}K^{-1}$)	$\beta \times 10^{-5}K^{-1}$
Base fluid (Kerosene Oil)	783	2090	0.145	99
Ag (s_1)	10500	235	429	1.89
Cu (s_2)	8993	385	401	1.67
TiO_2 (s_3)	4250	686.20	8.9538	0.90

The expressions for the thermophysical properties of the tri-hybrid nanofluid are shown below:

$$\rho_{nf} = \rho_f(1-\phi_1) + \phi_1(\rho_{s1})$$

$$\mu_{nf} = \frac{\mu_f}{(1-\varphi_1)^{2.5}}$$

$$(\rho C_p)_{nf} = (\rho C_p)_f(1-\phi_1) + \phi_1(\rho C_p)_{s1}$$

$$\frac{k_{nf}}{k_f} = \frac{k_{s1} + 2k_f - 2(k_f - k_{s1})\phi_1}{k_{s1} + 2k_f + \phi_1(k_f - k_{s1})}$$

$$\rho_{hnf} = (1-\phi_2)(\rho_f(1-\phi_1) + \phi_1\rho_{s1}) + \phi_2\rho_{s2}$$

$$\mu_{hnf} = \frac{\mu_f}{(1-\varphi_1)^{2.5}(1-\varphi_2)^{2.5}}$$

$$(\rho C_p)_{hnf} = \left((1-\phi_2)(\rho C_p)_f(1-\phi_1) + \phi_1(\rho C_p)_{s1}\right) + \phi_2(\rho C_p)_{s2}$$

$$\frac{k_{hnf}}{k_{hf}} = \frac{k_{s2}+2k_{nf}-2(k_{nf}-k_{s2})\phi_2}{k_{s2}+2k_{nf}+\phi_2(k_{nf}-k_{s2})},$$

$$\rho_{thnf} = (1-\phi_3)\left[(1-\phi_2)\left[(1-\phi_1)\rho_f + \phi_1\rho_{s1}\right] + \phi_2\rho_{s2}\right] + \phi_3\rho_{s3}$$

$$\mu_{thnf} = \frac{\mu_f}{(1-\varphi_1)^{2.5}(1-\varphi_2)^{2.5}(1-\varphi_3)^{2.5}}$$

$$(\rho C_p)_{thnf} = (1-\phi_3)[(1-\phi_2)\left((\rho C_p)_f(1-\phi_1) + \phi_1(\rho C_p)_{s1}\right) + \phi_2(\rho C_p)_{s2}] + \phi_3(\rho C_p)_{s3}$$

$$\frac{k_{thnf}}{k_{hnf}} = \frac{k_{s3} + 2k_{hnf} - 2(k_{hnf} - k_{s3})\phi_3}{k_{s3} + 2k_{hnf} + \phi_3(k_{hnf} - k_{s3})}.$$

Where $\phi 1$ and $\phi 2$ are volumetric solid proportion of nanoparticles, such as silver (Ag), Copper (Cu) and Titanium ($TiO2$) respectively. Here, 1, $s1$, and $s2$ are used to differentiate the heat related properties regarding base fluid and nanomaterials of the first kind (Ag), second kind (Cu) and third kind ($TiO2$).

Computational Strategy:

Equations (7–8), together with the boundary constraints specified in Eq. (9), are simplified numerically using the built-in MATLAB solver bvp4c. For this purpose, the governing higher-order ODEs in equations (7–8) are first shifted into first-order ODEs system. The resulting system, along with the associated boundary constraints given in (9), is

then implemented in the bvp4c framework to obtain the numerical solutions. The computational procedure is described as follows:

$$\phi(1) = \psi, \phi(2) = \psi', \phi(3) = \psi'', \phi(4) = \chi, \phi(5) = \chi' \tag{11}$$

$$\phi\phi 1 = \frac{\left(2\phi(2)^2 - \phi(1)\phi(3) + \frac{\lambda_1}{\frac{\rho_{hnf}}{\rho_f}}\left[\phi(2)^2\phi(3) + 2\phi(2)\left(\phi(1) + \eta\phi(2)\right)\phi(3)\right] - \frac{\frac{(\rho\beta_T)_{hnf}}{(\rho\beta_T)_f}}{\frac{\rho_{hnf}}{\rho_f}}\lambda\chi - \frac{\frac{\sigma_{hnf}}{\sigma_f}}{\frac{\rho_{hnf}}{\rho_f}}M\phi(2) + \frac{\mu_{hnf}}{\mu_f}K\phi(2) \right)}{\left(\frac{\frac{\mu_{hnf}}{\mu_f}}{\frac{\rho_{hnf}}{\rho_f}} - \frac{\lambda_1}{\frac{\rho_{hnf}}{\rho_f}}\left(\phi(1) + \eta\phi(2)\right)^2 \right)} \tag{12}$$

$$\phi\phi 2 = -\frac{Pr(\psi\chi' - \chi\psi')}{\frac{\frac{k_{hnf}}{k_f}}{\frac{(\rho C_p)_{hnf}}{(\rho C_p)_f}}} \tag{13}$$

Boundary conditions

$$\left.\begin{array}{l} \phi(1) = S,\ \phi(2) = 1,\ \phi(4) = 1,\ \text{at}\ \eta = 0 \\ \phi(2) \to 0,\ \phi(4) \to 0,\ \text{as}\ \eta \to \infty \end{array}\right\}. \tag{14}$$

Results and Discussion:

The results obtained using the principal numerical solution technique are illustrated in graphical and tabular forms as well. The profiles of ψ' and χ, representing the dimensionless velocity and temperature distributions, respectively, are illustrated graphically. In addition, the shear stress coefficient with respect to wall, $Re1/2Cf$, and the convective heat-transfer rate, $Re-1/2$Nu, are summarized in tabulated form. The numerical analysis is carried out for various governing parameters, including the Maxwell fluid parameter $\lambda 1$, magnetic/Lorentz force parameter M, buoyancy parameter λ, Prandtl number Pr, dimensionless porosity parameter K, and suction parameter S(S>0). The effects of these parameters on the velocity and temperature-dependent transport characteristics of the flow are systematically examined.

The involvement of M on the motion profile ψ' and temperature distribution χ is illustrated in Figure. 2 and Figure 3. It is evident that an increase in M suppresses the fluid velocity, whereas the temperature profile increases for both Ag/kerosene oil and Ag–Cu/kerosene oil nanofluids. As the magnetic-field intensity increases, the corresponding Lorentz force becomes stronger, thereby enhancing the resistance encountered by the fluid motion. Consequently, the velocity profile decreases due to the greater opposing electromagnetic force. At the same time, the associated resistive effects promote an increase in the thermal field, leading to a higher temperature distribution. Furthermore, the Ag/kerosene-oil nanofluid exhibits higher velocity profiles than the Ag–Cu/kerosene-oil hybrid nanofluid, whereas the temperature distribution, χ, demonstrates the reverse behavior.

Figure 4 illustrates the influence of the relaxation-time parameter $\lambda 1$, on the velocity profile, ψ'. It is clear that increasing $\lambda 1$ results to a noticeable rise in the flow velocity throughout the boundary layer. Moreover, over the complete computational structure, the Ag/kerosene-oil nanofluid shows a consistently higher velocity profile than the Ag–Cu/kerosene-oil nanofluid. Figure 5 presents the effect of the inclination angle, ξ, on the velocity distribution, ψ'. The results show a continuous enhancement in velocity as the inclination angle rises from ξ=0 to π/6, π/3, and π/2.

Figures 6 and 7 show the involvement of the permeable-medium K on ψ' and χ profiles.

The results demonstrate that enhancement in K leads to a pronounced reduction in the velocity distribution, showing that greater permeable-medium resistance increasingly restricts fluid motion. Moreover, the Ag/kerosene oil nanofluid maintains comparatively higher velocity profiles than the Ag–Cu/kerosene oil hybrid nanofluid. In contrast, the temperature profiles show the opposite behavior: an increase in K enhances the thermal distribution, with the Ag–Cu/kerosene oil configuration producing relatively higher profiles of temperature than the Ag/kerosene oil case.

Table 2 shows the effect of the permeability parameter K on the disseminate Nusselt number, $Re-1/2\mathrm{Nu}$, and the wall shear coefficient, $2Re1/2\ Cf$. The results show that increasing K leads to a simultaneous decrease in the reduced Nusselt number and an increase in the wall shear coefficient. Similarly, Table 3 presents the effect of the Prandtl number Pr on $2Re1/2\ Cf$ and $2Re-1/2\mathrm{Nu}$. It is observed that higher values of Pr progressively enhance the wall shear coefficient, whereas the reduced Nusselt number decreases accordingly.

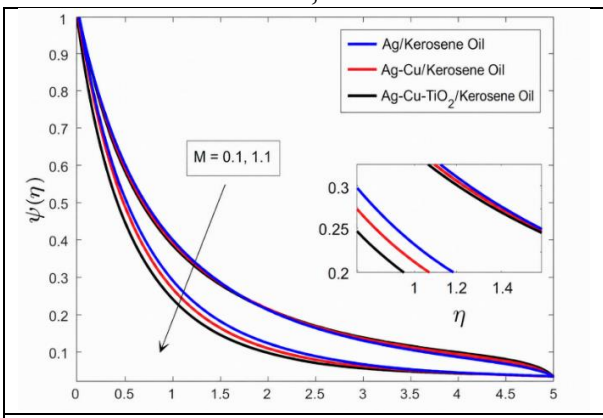

Figure 2. Fluctuation in ψ' relative to *M*
Pr=6.95, M=1.35; B = 0.135; Gr=0.135; K = 1.35; S=0.0;

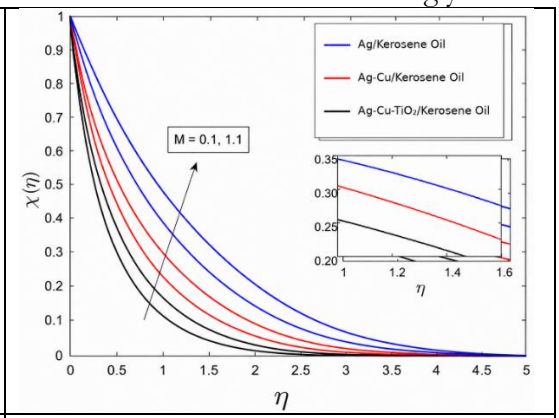

Figure 3. Fluctuation in ψ' relative to ***M***
Pr=6.95, M=1.35; B = 0.135; Gr=0.135; K = 1.35; S=0.0;

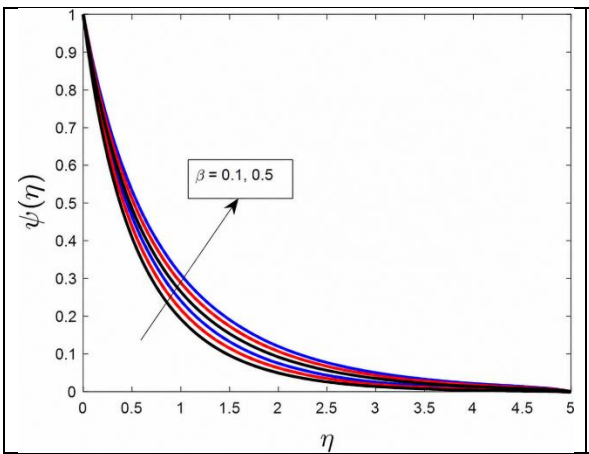

Figure 4. Fluctuation in χ relative to ***M***
Pr=6.95, M=1.35; B = 0.135; Gr=0.135; K = 1.35; S=0.0;

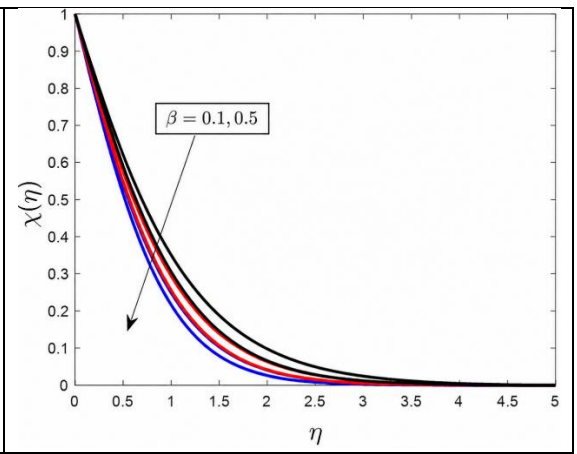

Figure .5 Fluctuation in ψ' relative to $\boldsymbol{\lambda 1}$
Pr=6.95, M=1.35; B = 0.135; Gr=0.135; K = 1.35; S=0.0;

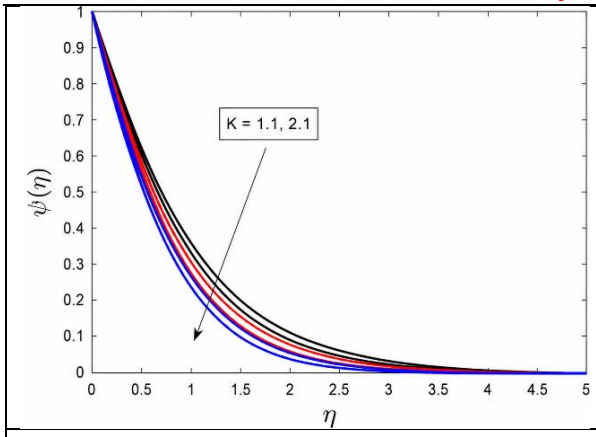

Figure 6. Fluctuation in χ relative to with ξ Pr=6.95, M=1.35; B = 0.135; Gr=0.135; K = 1.35; S=0.0;

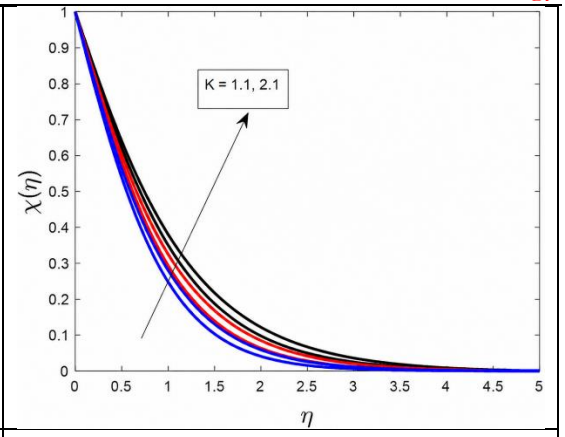

Figure 7. Fluctuation in ψ' relative to $\boldsymbol{K}$ Pr=6.95, M=1.35; B = 0.135; Gr=0.135; K = 1.35; S=0.0;

Table 2. Computational Results of $a)\ Re^{1/2}C_f b)\ Re^{-1/2}Nu$ *for* $M = 1.6$, $Pr = 7.0$, $\phi 1 = \phi 2 = 0.01$, $\lambda 1 = 0.1$, $\lambda = 0.1$, $\xi =$, $S = 0.2$ on contrast with Pr

K	$Re^{1/2}C_f$	$Re^{-1/2}Nu$
1.125	-1.454	2.6895
2.125	-1.7302	2.6424
3.125	-1.9743	2.6017
4.125	-2.1932	2.5655

Table 3. Computational Results of $a)\ Re^{1/2}C_f b)\ Re^{-1/2}Nu$ *for* $M = 0.75$, $K = 1.1$, $\phi 1 = \phi 2 = 0.01$, $\lambda 1 = 0.1$, $\lambda = 0.1$, $\xi = \pi$, $S = 0.2$ on contrast with Pr

Pr	$Re^{1/2}C_f$	$Re^{-1/2}Nu$
1.01	2.085	3.01
5.01	2.085	4.209
7.01	2.085	4.541
10.01	2.085	4.939

Practical Implications and Recommendations:

The present findings provide useful guidance for the design of thermal-management and cooling systems employing Ag–Cu–TiO_2/kerosene ternary hybrid nanofluids. The results indicate that wall suction can be used to control the boundary-layer thickness and improve surface heat removal, while the magnetic field provides an external mechanism for regulating fluid motion and thermal transport. However, excessively strong magnetic fields may suppress the velocity because of the increased Lorentz-force resistance.

Similarly, porous-medium resistance should be selected carefully, since greater flow resistance can reduce the fluid velocity and may increase the pumping requirement. Therefore, highly restrictive porous structures should be avoided when rapid coolant circulation is required. The addition of Ag, Cu, and TiO_2 nanoparticles enhances the thermal characteristics of kerosene oil, but the nanoparticle concentration should be optimized because excessive loading may increase viscosity and flow resistance. For practical applications, moderate magnetic-field strength, controlled suction, sufficiently high porous-medium permeability, and an optimized nanoparticle volume fraction are recommended to obtain a suitable balance between heat-transfer enhancement and hydrodynamic resistance. These observations may assist in the development of advanced cooling devices, heat exchangers, thermal-energy systems, and magnetically controlled thermal-management processes.

Conclusion:

In this paper, the effects of MHD forces and suction phenomenon on the fluid flow and thermal behavior of a ternary nano liquid, considered as an electrically conducting non-Newtonian fluid, flowing over a nonlinearly stretching flexible sheet immersed in a permeable medium, have been investigated. The main findings can be combining as follows:

The fluid motion rate increases with increasing values of inclination parameter, Maxwell relaxation parameter of Maxwell type, and suction-related negative parameter of pressure.

In contrast, the flow motion profile decreases as the permeable-resistance parameter and magnetic increase magnitude.

The temperature profile increases with increasing magnetic-field strength and higher permeable-medium resistance, while suction increasing intensity suppresses the temperature distribution.

A rise in the permeable-medium magnitude raised the skin-friction coefficient while reducing the dimensionless rate of heat transfer represented by the Nusselt number.

Similarly, an increase in the Prandtl number results in a continuous increase in skin friction, accompanied by a decrease in the Nusselt number.

All computed velocity and temperature profiles satisfy the prescribed boundary conditions and converge asymptotically toward the corresponding far-field values.

References:

[1] Animasaun, I.L.; Al-Mdallal, Q.M.; Khan, U.; Alshomrani, A.S, "Unsteady Water-Based Ternary Hybrid Nanofluids on Wedges by Bioconvection and Wall Stretching Velocity: Thermal Analysis and Scrutinization of Small and Larger Magnitudes of the Thermal Conductivity of Nanoparticles," *Mathematics*, vol. 10, no. 22, 2022, doi: https://doi.org/10.3390/math10224309.

[2] S. Nasir, S. Sirisubtawee, P. Juntharee, A. S. Berrouk, S. Mukhtar, and T. Gul, "Heat transport study of ternary hybrid nanofluid flow under magnetic dipole together with nonlinear thermal radiation," *Appl. Nanosci. 2022 129*, vol. 12, no. 9, pp. 2777–2788, Aug. 2022, doi: 10.1007/S13204-022-02583-7.

[3] M. Shanmugapriya, R. Sundareswaran, P. Senthil Kumar, and G. Rangasamy, "Impact of nanoparticle shape in enhancing heat transfer of magnetized ternary hybrid nanofluid," *Sustain. Energy Technol. Assessments*, vol. 53, p. 102700, Oct. 2022, doi: 10.1016/J.SETA.2022.102700.

[4] M. Arif, P. Kumam, W. Kumam, and Z. Mostafa, "Heat transfer analysis of radiator using different shaped nanoparticles water-based ternary hybrid nanofluid with applications: A fractional model," *Case Stud. Therm. Eng.*, vol. 31, p. 101837, Mar. 2022, doi: 10.1016/J.CSITE.2022.101837.

[5] I. Zahan, R. Nasrin, and S. Khatun, "Thermal performance of ternary-hybrid nanofluids through a convergent-divergent nozzle using distilled water - ethylene glycol mixtures," *Int. Commun. Heat Mass Transf.*, vol. 137, p. 106254, Oct. 2022, doi: 10.1016/J.ICHEATMASSTRANSFER.2022.106254.

[6] P. Priyadharshini, M. V. Archana, N. A. Shah, and M. H. Alshehri, "Ternary Hybrid Nanofluid Flow Emerging on a Symmetrically Stretching Sheet Optimization with Machine Learning Prediction Scheme," *Symmetry 2023, Vol. 15, Page 1225*, vol. 15, no. 6, p. 1225, Jun. 2023, doi: 10.3390/SYM15061225.

[7] J. K. Madhukesh, I. E. Sarris, B. C. Prasannakumara, and A. Abdulrahman, "Investigation of Thermal Performance of Ternary Hybrid Nanofluid Flow in a Permeable Inclined Cylinder/Plate," *Energies 2023, Vol. 16, Page 2630*, vol. 16, no. 6, p. 2630, Mar. 2023, doi: 10.3390/EN16062630.

[8] M. Arif, L. Di Persio, P. Kumam, W. Watthayu, and A. Akgül, "Heat transfer analysis of fractional model of couple stress Casson tri-hybrid nanofluid using dissimilar shape

nanoparticles in blood with biomedical applications," *Sci. Reports 2023 131*, vol. 13, no. 1, pp. 4596-, Mar. 2023, doi: 10.1038/s41598-022-25127-z.

[9] M. Z. Ullah, "Irreversibility Marangoni Tri-Hybrid Nanoflow Analysis for Thermal Enhancement Applications," *Nanomater. 2023, Vol. 13, Page 423*, vol. 13, no. 3, p. 423, Jan. 2023, doi: 10.3390/NANO13030423.

[10] V. Rajesh and M. Sheremet, "Natural Convection of Ternary Hybrid Nanofluid in a Differential-Heated Enclosure with Non-Uniform Heating Wall," *Micromachines 2023, Vol. 14, Page 1049*, vol. 14, no. 5, p. 1049, May 2023, doi: 10.3390/MI14051049.

[11] M. Mahboobtosi, K. Hosseinzadeh, and D. D. Ganji, "Entropy generation analysis and hydrothermal optimization of ternary hybrid nanofluid flow suspended in polymer over curved stretching surface," *Int. J. Thermofluids*, vol. 20, p. 100507, Nov. 2023, doi: 10.1016/J.IJFT.2023.100507.

[12] M. Mumtaz, S. Islam, H. Ullah, and Z. Shah, "Chemically reactive MHD convective flow and heat transfer performance of ternary hybrid nanofluid past a curved stretching sheet," *J. Mol. Liq.*, vol. 390, p. 123179, Nov. 2023, doi: 10.1016/J.MOLLIQ.2023.123179.

[13] A. A. Alharbi, "Thermal analysis of heat transport in a slip flow of ternary hybrid nanofluid with suction upon a stretching/shrinking sheet," *Case Stud. Therm. Eng.*, vol. 54, p. 103965, Feb. 2024, doi: 10.1016/J.CSITE.2023.103965.

[14] Shilpa, R. Mehta, and K. Senthilvadivu, "Artificial neural network analysis on heat and mass transfer in MHD Carreau ternary hybrid nanofluid flow across a vertical cylinder: A numerical computation," *Int. J. Thermofluids*, vol. 27, p. 101171, May 2025, doi: 10.1016/J.IJFT.2025.101171.

[15] A. M. Obalalu, U. Khan, E. O. Fatunmbi, N. S. Khashi'ie, and J. A. Bashatah, "MHD heat and mass transfer of a ternary hybrid nanofluid over a rotating sphere," *Discov. Nano 2026 211*, vol. 21, no. 1, pp. 163-, May 2026, doi: 10.1186/S11671-026-04597-4.

[16] K. A. M. Alharbi *et al.*, "Computational Valuation of Darcy Ternary-Hybrid Nanofluid Flow across an Extending Cylinder with Induction Effects," *Micromachines 2022, Vol. 13, Page 588*, vol. 13, no. 4, p. 588, Apr. 2022, doi: 10.3390/MI13040588.

[17] M. Bilal *et al.*, "Numerical Analysis of an Unsteady, Electroviscous, Ternary Hybrid Nanofluid Flow with Chemical Reaction and Activation Energy across Parallel Plates," *Micromachines 2022, Vol. 13, Page 874*, vol. 13, no. 6, p. 874, May 2022, doi: 10.3390/MI13060874.

[18] M. Nagapavani, G. Venkata Ramana Reddy, A. Verma, R. Mishra, and T. Kumar, "Significance of Arrhenius activation energy and binary chemical reaction in ternary hybrid nanofluid flow over a convectively heated porous curved surface: A passive control strategy," *Int. J. Mod. Phys. B*, vol. 37, no. 25, Oct. 2023, doi: 10.1142/S0217979223502910.

[19] B. Ali, S. Jubair, A. Aluraikan, M. A. El-Rahman, S. M. Eldin, and H. Abd El-Wahed Khalifa, "Numerical investigation of heat source induced thermal slip effect on trihybrid nanofluid flow over a stretching surface," *Results Eng.*, vol. 20, p. 101536, Dec. 2023, doi: 10.1016/J.RINENG.2023.101536.

[20] S. Murtaza, P. Kumam, T. Sutthibutpong, P. Suttiarporn, T. Srisurat, and Z. Ahmad, "Fractal-fractional analysis and numerical simulation for the heat transfer of ZnO + Al2O3 + TiO2/DW based ternary hybrid nanofluid," *ZAMM - J. Appl. Math. Mech. / Zeitschrift für Angew. Math. und Mech.*, vol. 104, no. 2, p. e202300459, Feb. 2024, doi: 10.1002/ZAMM.202300459.

[21] F. A. Shah, T. Zamir, N. S. Akbar, and A. Mikhaylov, "Levenberg-marquardt design for analysis of maxwell fluid flow on ternary hybrid nanoparticles passing over a riga plate under convective boundary conditions," *Results Eng.*, vol. 24, p. 103502, Dec.

2024, doi: 10.1016/J.RINENG.2024.103502.

[22] M. Mahboobtosi, K. Hosseinzadeh, and D. D. Ganji, "Investigating the convective flow of ternary hybrid nanofluids and single nanofluids around a stretched cylinder: Parameter analysis and performance enhancement," *Int. J. Thermofluids*, vol. 23, p. 100752, Aug. 2024, doi: 10.1016/J.IJFT.2024.100752.

[23] N. S. Wahid, N. M. Arifin, R. I. Yahaya, N. S. Khashi'ie, and I. Pop, "Impact of suction and thermal radiation on unsteady ternary hybrid nanofluid flow over a biaxial shrinking sheet," *Alexandria Eng. J.*, vol. 96, pp. 132–141, Jun. 2024, doi: 10.1016/J.AEJ.2024.03.079.

[24] H. AL Garalleh, "Numerical simulation of heat transport mechanism in chemically influenced ternary hybrid nanofluid flow over a wedge geometry," *Discov. Appl. Sci. 2024 69*, vol. 6, no. 9, pp. 449-, Aug. 2024, doi: 10.1007/S42452-024-06141-4.

[25] A. U. Hayat, H. Khan, I. Ullah, H. Ahmad, M. M. Alam, and M. Bilal, "Numerical exploration of the entropy generation in tri-hybrid nanofluid flow across a curved stretching surface subject to exponential heat source/sink," *J. Therm. Anal. Calorim. 2024 14917*, vol. 149, no. 17, pp. 10017–10029, Jul. 2024, doi: 10.1007/S10973-024-13358-3.

[26] S. Dey, S. Ontela, P. K. Pattnaik, and S. R. Mishra, "Convective heat transfer of tri-hybrid nanofluid through a curved expanding surface with the impact of velocity slip and exponential heat source," *Colloid Polym. Sci. 2024 30210*, vol. 302, no. 10, pp. 1573–1590, Jul. 2024, doi: 10.1007/S00396-024-05291-6.

[27] M. Mumtaz, "Hydrothermal dynamics of darcy Forchheimer ternary hybrid nanofluid flow past bended surface with active—passive controls," *Adv. Mech. Eng.*, vol. 16, no. 10, Oct. 2024, doi: 10.1177/16878132241293958;

[28] S. Z. Hussain Shah, A. Ayub, U. Khan, A. Darvesh, E. S. M. Sherif, and I. Pop, "Thermal transport exploration of ternary hybrid nanofluid flow in a non-Newtonian model with homogeneous-heterogeneous chemical reactions induced by vertical cylinder," *Adv. Mech. Eng.*, vol. 16, no. 5, May 2024, doi: 10.1177/16878132241252229;

[29] S. K. Rawat *et al.*, "Designing artificial intelligence computing techniques to study heat transfer of a ternary hybrid nanofluid flow: Application of particle swarm optimization and artificial neural network," *MPLB*, vol. 39, no. 24, pp. 2550114–105, Aug. 2025, doi: 10.1142/S0217984925501143.

[30] A. B. Sadiya and G. Sucharitha, "Computational analysis of MHD ternary hybrid nanofluid flow with thermochemical reactions through a porous medium on a rotating stretching sheet," *Discov. Nano 2025 201*, vol. 20, no. 1, pp. 168-, Sep. 2025, doi: 10.1186/S11671-025-04353-0.

[31] T. Sindhu and K. Jagadeeshkumar, "Entropy generation and regression analysis of unsteady Carreau ternary hybrid nanofluid flow with electromagnetic and thermal influences," *Discov. Nano 2025 201*, vol. 20, no. 1, pp. 231-, Dec. 2025, doi: 10.1186/S11671-025-04408-2.

[32] N. Sarwar, S. Jahangir, M. I. Asjad, and S. M. Eldin, "Application of Ternary Nanoparticles in the Heat Transfer of an MHD Non-Newtonian Fluid Flow," *Micromachines 2022, Vol. 13, Page 2149*, vol. 13, no. 12, p. 2149, Dec. 2022, doi: 10.3390/MI13122149.

Copyright © by authors and 50Sea. This work is licensed under Creative Commons Attribution 4.0 International License.